INTERFACE FOCUS

rsfs.royalsocietypublishing.org

Research

Cite this article: Connizzo BK, Han L, Birk DE, Soslowsky LJ. 2016 Collagen V-heterozygous and -null supraspinatus tendons exhibit altered dynamic mechanical behaviour at multiple hierarchical scales. *Interface Focus* **6**: 20150043. http://dx.doi.org/10.1098/rsfs.2015.0043

One contribution of 19 to a theme issue 'Integrated multiscale biomaterials experiment and modelling: towards function and pathology'.

Subject Areas:
bioengineering

Keywords:
tendon, multiscale mechanics, Ehlers–Danlos syndrome, supraspinatus, re-alignment, fibril sliding

Author for correspondence:
Louis J. Soslowsky
e-mail: soslowsk@upenn.edu

Collagen V-heterozygous and -null supraspinatus tendons exhibit altered dynamic mechanical behaviour at multiple hierarchical scales

Brianne K. Connizzo[1], Lin Han[2], David E. Birk[3] and Louis J. Soslowsky[1]

[1]McKay Orthopaedic Research Laboratory, University of Pennsylvania, 424 Stemmler Hall, 36th and Hamilton Walk, Philadelphia, PA 19104-6081, USA
[2]School of Biomedical Engineering, Science and Health Systems, Drexel University, 3141 Chestnut Street, Philadelphia, PA 19104, USA
[3]Department of Molecular Pharmacology and Physiology, Morsani College of Medicine, University of South Florida, Tampa, FL 33612, USA

Tendons function using a unique set of mechanical properties governed by the extracellular matrix and its ability to respond to varied multi-axial loads. Reduction of collagen V expression, such as in classic Ehlers–Danlos syndrome, results in altered fibril morphology and altered macroscale mechanical function in both clinical and animal studies, yet the mechanism by which changes at the fibril level lead to macroscale functional changes has not yet been investigated. This study addresses this by defining the multiscale mechanical response of wild-type, collagen V-heterozygous and -null supraspinatus tendons. Tendons were subjected to mechanical testing and analysed for macroscale properties, as well as microscale (fibre re-alignment) and nanoscale (fibril deformation and sliding) responses. In many macroscale parameters, results showed a dose-dependent response with severely decreased properties in the null group. In addition, both heterozygous and null groups responded to load faster than in wild-type tendons via earlier fibre re-alignment and fibril stretch. However, the heterozygous group exhibited increased fibril sliding, while the null group exhibited no fibril sliding. These studies demonstrate that dynamic responses play an important role in determining overall function and that collagen V is a critical regulator in the development of these relationships.

1. Introduction

Tendons function to stabilize the skeleton and allow efficient transfer of energy through their unique set of mechanical properties. The primarily uniaxial tensile function along the longitudinal axis of its collagen fibres enables transmission of generated muscle force to bone. Tendon exhibits nonlinear biomechanical behaviour as exhibited by a typical stress–strain curve with an initial, nonlinear 'toe-region' followed by the 'linear-region' [1]. This nonlinearity, in particular the low stiffness toe-region, is thought to be attributed to a number of dynamic microstructural re-arrangements [1–8]. Particularly, the flattening or disappearance of the collagen fibre crimp morphology has been implicated in the nonlinear behaviour observed in the toe-region [9,10]. In addition, re-orientation of collagen fibres towards the axis of mechanical load also has been found to occur during this period. Macroscopic tendon extension is also enabled by deformation and sliding mechanisms that simultaneously occur between fibres and between fibrils within each fibre [8,11,12]. In addition to their anisotropic and nonlinear behaviour, tendons exhibit several viscoelastic properties, such as stress relaxation, hysteresis and creep [2,13–19]. This process is both static and dynamic, as demonstrated by a similar decrease in peak stress over time with repetitive, cyclic tensile loading [20]. Fibril sliding has also been cited as a contributor to dynamic viscoelastic behaviour during

THE ROYAL SOCIETY PUBLISHING

this initial response to load [19]. These viscoelastic properties emphasize the ability of tendon to structurally adapt to constant or cyclical loads in order to reach biomechanical equilibrium [21].

Tendon's unique set of mechanical properties is controlled by the location-dependent and site-dependent composition and structure of the tissue, primarily by its extracellular matrix. This matrix, comprised predominantly of collagen type I, is organized in a hierarchical manner parallel to the mechanical axis of the tendon [22–25]. In addition to collagen I, the extracellular matrix is composed of quantitatively minor collagens, elastin and fibrillins, proteoglycans (PGs) and their glycosaminoglycan chains, glycolipids, and cellular material [26]. The development of this unique structure is modulated mainly by PGs and minor collagens, such as collagen types V, XI, XII and XIV. Collagen V, although a quantitatively minor component (approx. 2%) in mature tendon and ligament composition, is a major regulator of fibrillogenesis. Collagen V plays a critical role during the early process of fibril nucleation and reduction of collagen V expression during this process results in fewer collagen I fibrils with increased diameters in tendons, ligaments, dermis and cornea [27–31].

A clinical representation of collagen V reduction is the classic form of Ehlers–Danlos syndrome (EDS), with more than 50% of patients being haploinsufficient for COL5A1 [32,33]. These patients exhibit hyperextensible skin, joint hypermobility and instability, as well as abnormal wound healing and scarring, suggesting a crucial role for collagen V in both structure and function of tendons and ligaments. Recent studies with both an established haploinsufficient *Col5a1*$^{+/-}$ *classic* EDS mouse model and a tendon/ligament-specific collagen V-null model have demonstrated altered fibril structure and inadequate macroscale tensile mechanical function [28,29,31,34]. In addition, evidence suggests that the role of collagen V in establishing tendon mechanical properties is tissue-specific, alluding to a limited understanding of the mechanisms by which structure relates to mechanical function. The goal of this study is to define the relationship between hierarchical collagen structure and function by evaluating the dynamic mechanical properties of collagen V heterozygous and null tendons at a hierarchy of length scales, including fibril, fibre and whole-tissue levels. We hypothesized that collagen V deficiency would result in impaired dynamic mechanical function at all length scales, with a stronger phenotype in the null than heterozygous mice. We also hypothesized that changes in dynamic responses at nanoscale (fibril) and microscale (fibre) (collagen re-alignment, deformation, sliding) are more apparent than those at the tissue level, and can be used to interpret the tissue-level changes.

2. Material and methods

Three hundred male mice from three different groups were used in this IACUC-approved study: C57BL/6 control (WT), Col5a1$^{+/-}$ (HET) and a tendon/ligament-specific collagen V-null model, Col5a1$^{\Delta ten/\Delta ten}$ (NULL) [31,35]. Mice were bred to 120 days of age and sacrificed humanely, at which point shoulders were frozen at −20°C until dissection for mechanical testing. To prepare tendons for mechanical testing, supraspinatus (SST) tendons were dissected from the shoulder and surrounding soft tissue was carefully removed [6,36]. Tendon cross-sectional area was measured using a laser-based device and Verhoeff's stain lines were applied for optical tracking [36–39]. The humerus was fixed in a polymethylmethacrylate pot while the tendon was positioned between a sandpaper–cyanoacrylate construct. Both sides were then placed in custom grips for testing with a gauge length of 2.5 mm. All analyses below were performed at both the insertion site and midsubstance of the SST tendon.

2.1. Dynamic viscoelastic testing

Twenty specimens from each group designated for dynamic viscoelastic testing were subjected to a testing protocol as described previously [13,14,40]. Tendons were first preloaded and preconditioned for 10 cycles to 1.5% grip strain at 0.25 Hz. Following a 5 min hold, tendons underwent three stress relaxations (to 4, 6 and 8% grip strain) at 5% s^{-1} with sinusoidal frequency sweeps superimposed upon the static strain. Each frequency sweep consists of 10 cycles of 0.125% amplitude sinusoidal grip strain at frequencies of 0.1, 1 and 10 Hz. The tendons were then returned to zero displacement and then subjected to a final ramp to failure at 0.05% s^{-1}. Images were captured during the ramp to failure and analysed for standard tensile mechanical properties using optical tracking using custom software (Matlab, Natick, MA, USA), as described previously [36,40,41]. A bilinear curve fit was also applied to the optical stress–strain data to quantify transition stress, transition strain and the moduli in the toe and linear regions. In addition, the dynamic modulus $|E^*|$ (defined as the stress amplitude divided by the strain amplitude) and the phase angle δ (between the stress and strain) were computed at each frequency and strain level. The dynamic modulus ($|E^*|$) represents how difficult the material is to deform under dynamic loading, while the tangent of the phase angle ($\tan\delta$) is the ratio of loss over storage moduli [13,14,40,42]. Comparisons were made using one-way ANOVA for each parameter with post-hoc Bonferroni tests to correct for family-wise error associated with multiple comparisons.

2.2. Fatigue testing

An additional twenty specimens from each group were subjected to a fatigue loading protocol, as described previously [20,43]. Preliminary studies determined that the mean failure loads were significantly different between groups and as a result, all tendons were fatigue tested at 1 Hz between 20 and 75% of their ultimate failure load (0.75–2.75 N for wild-type and heterozygous groups, 0.25–1.0 N for the null group). As described previously, several parameters were computed: (i) maximum cyclic strain, (ii) tangent stiffness (calculated as the slope between the maximum and minimum force and displacements for each cycle), (iii) hysteresis (defined as the area enclosed by the stress–strain curve for a cycle), (iv) damage (defined as the ratio of displacement and gauge length at a set threshold to the tissue displacement and displacement at a set threshold after the first cycle of fatigue loading), and (v) cycles to failure (defined as the number of cycles until specimen failure) [43–45]. Comparisons were made using one-way ANOVA for each parameter with post-hoc Bonferroni tests.

2.3. Collagen fibre re-alignment

Collagen fibre re-alignment ($n = 20$/group) was quantified during the dynamic viscoelastic testing using our established integrated cross-polarizer technique [46–50]. At several points during the mechanical test (before and after preconditioning, before and after each stress relaxation event and throughout the ramp to failure), sets of 13 images were acquired as the polarizers rotate through a 125° range for calculation of fibre alignment. Comparisons of circular standard deviation, a measure of the spread of the distribution of fibre angles [4,5,46], was used to determine whether significant re-alignment occurred during each portion of

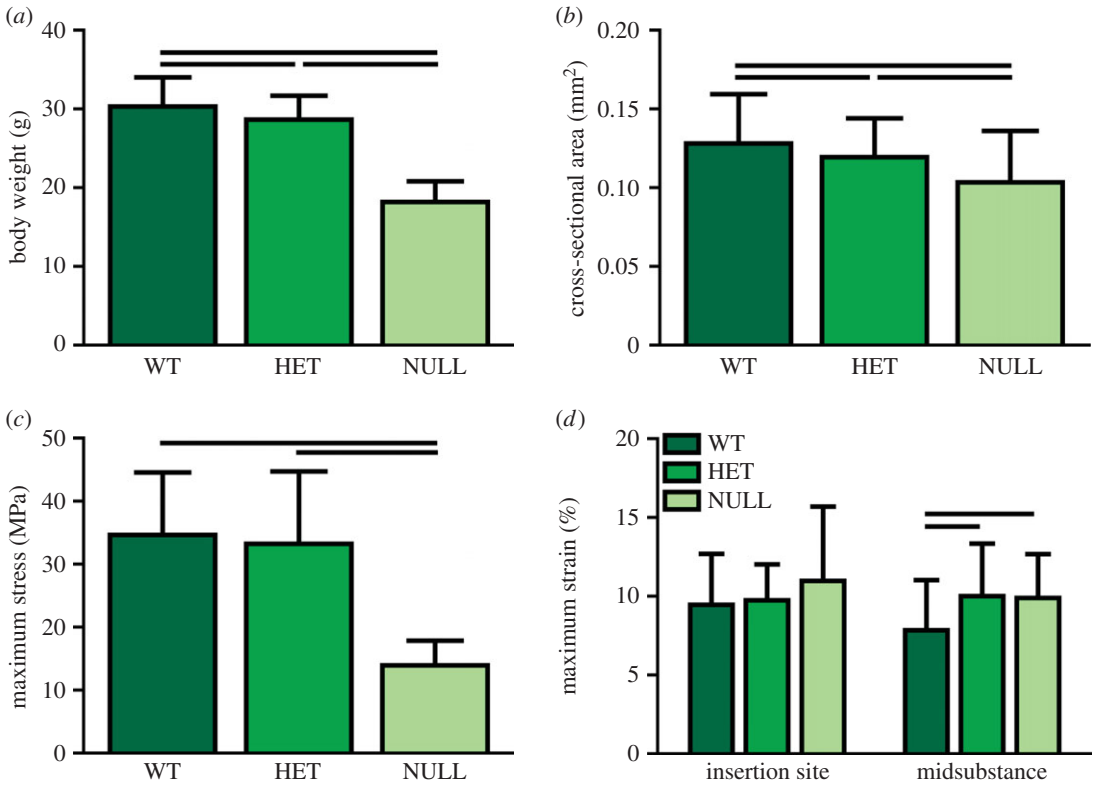

Figure 1. (*a*) Body weight and (*b*) tendon cross-sectional area were significantly reduced in both the heterozygous and null groups compared to the wild-type group. (*c*) Maximum stress reduced only in the null group, but both groups exhibited increased (*d*) maximum strain. Data are reported at mean ± s.d. (Online version in colour.)

the mechanical test. Statistical comparisons between regions of the mechanical test were made using non-parametric Kruskal–Wallis tests at each location. Re-alignment during the stress relaxation tests was split into two parameters. The first compared the change in circular standard deviation between 0% (after preconditioning) and 4% peak strain time point, which represent toe region strain levels (Toe Re-Alignment). The second compared the circular standard deviation between 4% peak strain and 8% peak strain, which represent linear region strain levels (Linear Re-Alignment). In addition, re-alignment during the ramp to failure exhibited bilinear behaviour with a linear decrease in circular standard deviation followed by a plateau. The strain required to reach the plateau and the amount of re-alignment that occurred (change in circular standard deviation) were measured for each specimen using a bilinear curve fit. Statistical comparisons were made between these measures using one-way ANOVA for each parameter with post-hoc Bonferroni tests.

2.4. Fibril deformation and sliding

Samples for collagen fibril deformation/sliding were prepared for mechanical testing and subjected to a standard preload and preconditioning prior to the ramp to failure. Tendons were then divided into five groups and stretched to a randomly assigned grip-to-grip strain value (0, 1, 3, 5 or 7%) at a rate of 0.1% strain per second. Tendons were then immediately frozen using freezing spray, placed in a specimen dish with tissue freezing medium, and submerged in liquid nitrogen [6,48]. Samples were frozen sectioned at 20 µm and immersed in cold 10% neutral buffered formalin for 4 min for fixation. For analysis of fibril deformation and sliding, imaging of 2 × 2 µm regions was performed by tapping mode imaging using NCHV-A probes (nominal spring constant $k \approx 42\ \mathrm{N\ m^{-1}}$, radius $R \approx 10$ nm) and a Dimension Icon AFM (BrukerNano, Santa Barbra, CA, USA) using a modified protocol described previously [6,8,51]. Tendons were scanned at two to three regions across the width of the insertion site and midsubstance of the tendon, and from four to six sections throughout the depth of the tendon. Custom software allowed for the measurement of *d*-period length for many fibrils in a single image [6]. Variability between and within specimens was determined to not be significantly different, and therefore fibrils were pooled across approximately five specimens sampled per strain level per group. Median and variance were obtained from fibril *d*-period distributions. Fibril stretch was calculated by subtracting the *d*-period length at each applied strain level by the initial *d*-period length. A change in fibril *d*-period variance from one strain to the next is indicative of strain heterogeneity between fibrils, or fibril sliding [6]. Statistical comparisons of *d*-period length across different strains were made using non-parametric Kruskal–Wallis tests followed by post-hoc Dunn's tests between strain levels. Comparisons of variance across strain levels were performed using a Bartlett test for unequal variances at each location with post-hoc *F*-tests between strain levels. For all statistical comparisons in this study, a *p*-value of $p < 0.05$ was considered statistically significant.

3. Results

3.1. Tissue-level quasi-static and dynamic viscoelastic mechanics

Body weight (figure 1*a*) and whole tendon cross-sectional area (figure 1*b*) were significantly reduced in the heterozygous and null groups compared to the wild-type group. Maximum load (not shown) and maximum stress were also significantly reduced in the null group, but there were no differences between the heterozygous and wild-type groups (figure 1*c*). Maximum tissue strain, determined optically, also was increased in both groups at the midsubstance, but not at the insertion site (figure 1*d*). Transition strain was not different

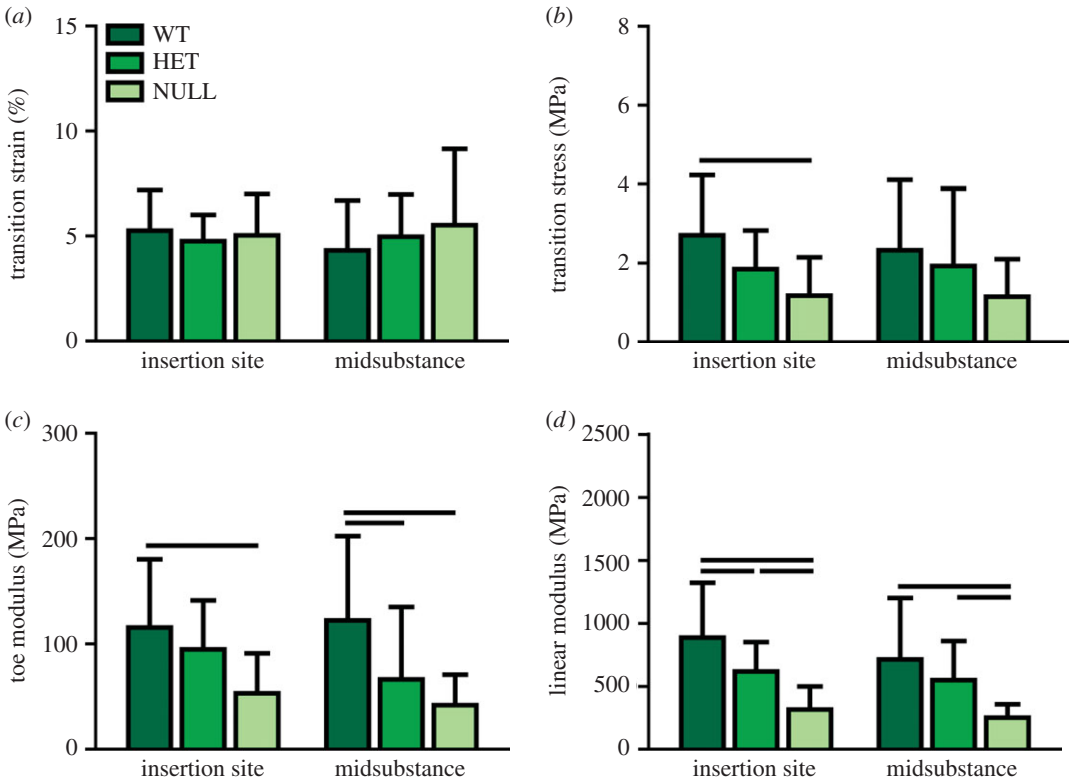

Figure 2. There were no differences in (*a*) transition strain between experimental groups, but (*b*) transition stress was significantly reduced in the null group at the insertion site. (*c*) Toe modulus was reduced in the null group at both sites and in the heterozygous group at the midsubstance. (*d*) Linear modulus was reduced in the null group at both sites and in the heterozygous group at the insertion site. Data are reported at mean ± s.d. (Online version in colour.)

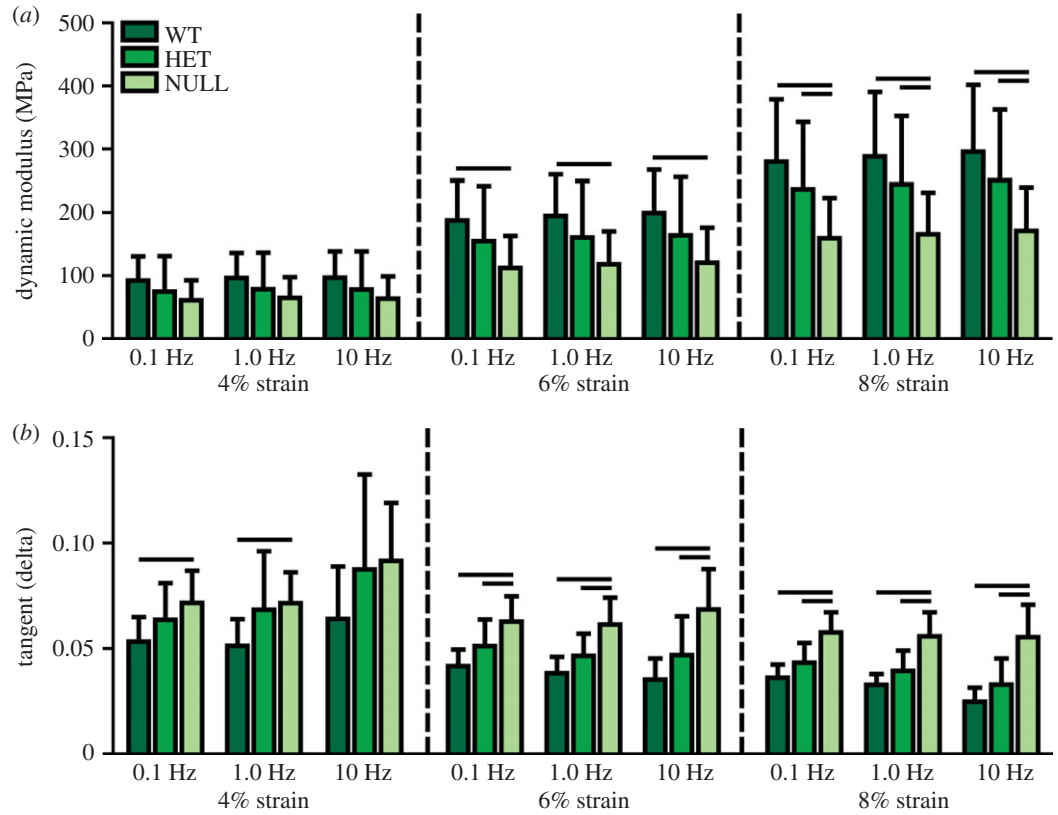

Figure 3. (*a*) Dynamic modulus was reduced in the null group at all frequencies at 6 and 8% strain. (*b*) Tangent delta was increased in the null group at all strains and frequencies except at 4% strain and 10 Hz. Data are reported at mean ± s.d. (Online version in colour.)

between the groups in either region (figure 2*a*), but transition stress was significantly less in the null group than the wild-type group at the insertion site (figure 2*b*). The moduli in both toe and linear regions were reduced in the null group at both sites (figure 2*c*,*d*). The heterozygous group also exhibited reduced toe modulus at the midsubstance and reduced linear modulus at the insertion site (figure 2*c*,*d*). Dynamic modulus increased and tangent delta decreased with increasing strain level as previously reported (figure 3). Dynamic modulus was significantly reduced in the null group at all frequencies

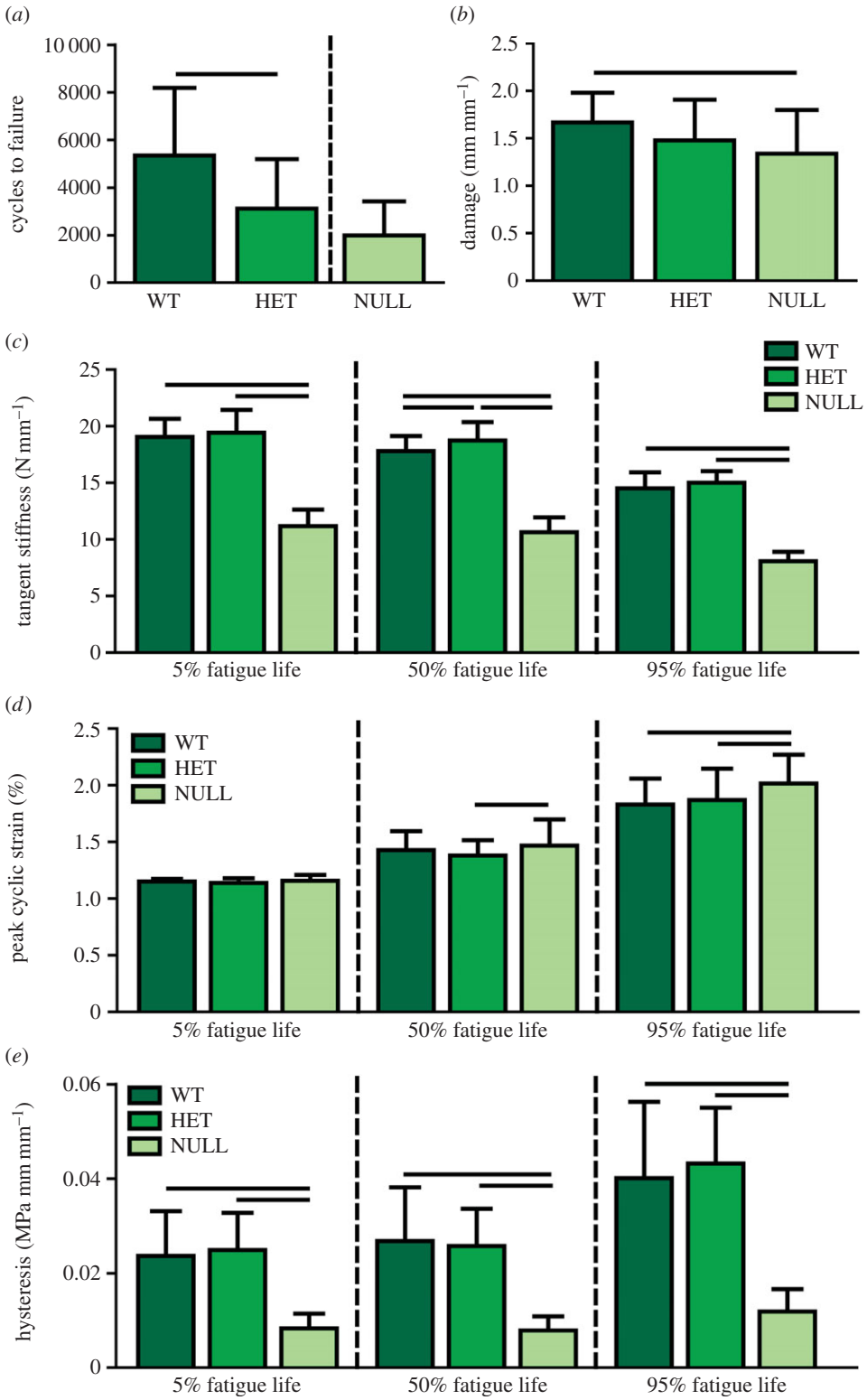

Figure 4. (*a*) The heterozygous group exhibited significantly decreased cycles to failure compared to the wild-type group. No statistical comparison was made with the null group due to protocol differences. (*b*) Damage was decreased in the null group at 5% fatigue life. (*c*) Tangent stiffness was decreased in the null group throughout fatigue life and increased in the heterozygous group at 50% fatigue life. (*d*) Peak cyclic strain was increased in the null group at 50 and 95% fatigue life. (*e*) Hysteresis was significantly reduced in the null group throughout fatigue life. Data are reported at mean ± s.d. (Online version in colour.)

compared to the wild-type group at both 6 and 8% strain and compared to the heterozygous group at 8% strain (figure 3*a*). Tangent delta of the null group was significantly greater than both the wild-type and heterozygous groups at all frequencies at both 6 and 8% strain levels (figure 3*b*). At 4% strain, the null and heterozygous groups were no different and the null group was higher than the wild-type group at 0.1 and 1.0 Hz. Finally, failure generally occurred at the insertion site, at the midsubstance or just below the top grip. The null tendons failed least often at the insertion site, while the other two groups displayed failure at all three locations equally.

3.2. Tissue-level fatigue mechanics

The heterozygous group exhibited approximately 40% fewer cycles to failure than the wild-type group (figure 4*a*). No statistical comparisons were made between the null group and other groups because the loading protocols were different,

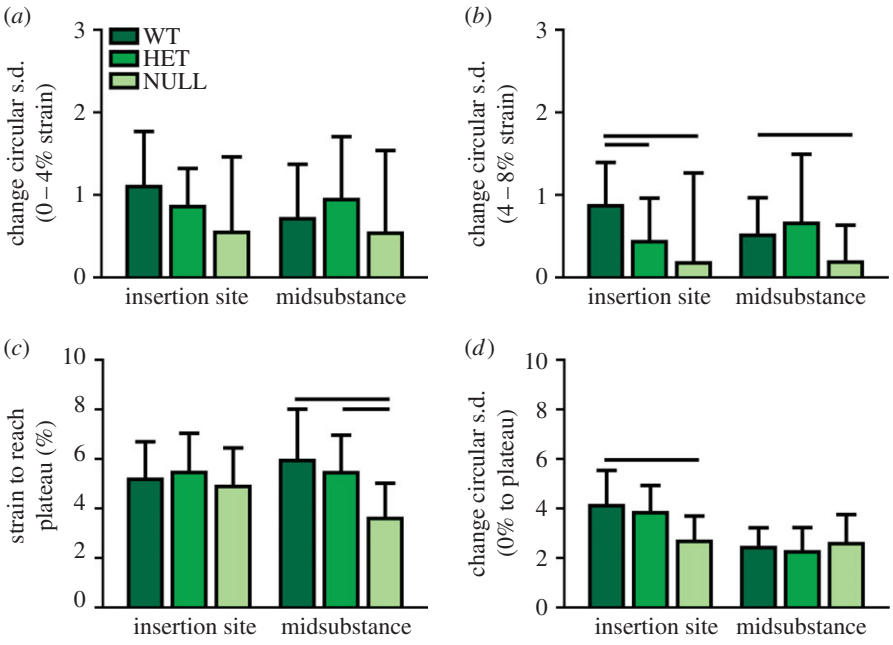

Figure 5. (*a*) Re-alignment in the toe region (0–4% strain) was not significantly different between groups, but (*b*) re-alignment in the linear region (4–8% strain) was reduced in the null group at both sites and in the heterozygous group at the insertion site. (*c*) The null group required less strain overall to fully re-align at the midsubstance and (*d*) re-aligned less overall at the insertion site. Data are reported at mean ± s.d. (Online version in colour.)

but the null group was lower than both other groups. Damage was significantly decreased only in the initial phase (5%) of fatigue life in the null group (figure 4*b*). Peak cyclic strain and damage increased while tangent stiffness and hysteresis decreased throughout fatigue life, as previously reported [20,43]. The null group had a significantly increased peak cyclic strain than the heterozygous group at 50% and both groups at 95% fatigue life (figure 4*d*). Tangent stiffness was reduced in the null group compared with the other groups at all three points in fatigue life (figure 4*c*). The heterozygous group also had an increased tangent stiffness when compared with the wild-type group at 50% fatigue life. Hysteresis was significantly reduced in the null group when compared with the wild-type and heterozygous groups at all three stages of fatigue life (figure 4*e*).

3.3. Collagen fibre re-alignment

In both the insertion and midsubstance of the wild-type groups, re-alignment occurred first following an increase in strain applied to the tissue (after the peak of stress relaxation events at 4, 6 and 8% strain). At the insertion site, the collagen fibres of the heterozygous and null groups re-aligned after the first two strain levels, but not with the final strain increase at 8% strain (data not shown). At the midsubstance, the heterozygous group re-aligned initially during the preconditioning and then again during each subsequent strain level, whereas the null group again only re-aligned after the addition of 4 and 6% strain. This is evidenced by comparing the circular standard deviation between 0 and 4% strain (figure 5*a*) to denote toe region re-alignment, which occurs in all groups, and between 4 and 8% strain (figure 5*b*) to denote linear region alignment, which is reduced in the null and heterozygous groups than in the wild-type group. All of the groups returned to a more disorganized state with the removal of strain (at the return to zero following the last stress relaxation) and then re-aligned again during the ramp to failure. However, the null group re-aligned fully at an earlier strain than both the heterozygous and wild-type groups at the midsubstance (figure 5*c*) and re-aligned less over that time period than the wild-type group at the insertion site (figure 5*d*).

3.4. Fibril deformation

Fibril *d*-period at 0% strain in the heterozygous group was increased at the insertion site and decreased at the midsubstance compared with both other groups (data not shown). Differential fibril deformation was observed at the insertion compared to the midsubstance. At the insertion site of the wild-type tendons, collagen fibril *d*-period showed a bimodal response, with an initial hold to 1% applied strain, followed by another increase at 5% applied strain with a decrease in *d*-period between them at 3% applied strain (figure 6*a*). At the midsubstance of the tissue, the fibril *d*-period increased monotonically, peaking at 3% applied strain and decreasing following to 7% strain (figure 6*a*(ii)). In the heterozygous group, the insertion site showed a similar trend to the wild-type group, but with a larger decrease at 3% applied strain (figure 6*b*). At the midsubstance, the heterozygous group showed an initial increase in *d*-period at 1 and 3% applied strain, but this was followed by no change in *d*-period length rather than the typical decrease attributed to fibril failure (figure 6*b*(ii)). In addition, initial fibril *d*-period in the heterozygous group was increased at the insertion site and decreased at the midsubstance when compared with the other groups. At the insertion site of the null group, there was an initial decrease in fibril *d*-period at 1% applied strain followed by an increase at 3% applied strain and a decrease thereafter (figure 6*c*(i)). At the midsubstance, the null tendon *d*-period initially decreased at 1% and increased thereafter with no apparent decrease in fibril *d*-period near the end of the test (figure 6*c*(ii)).

3.5. Fibril sliding

Fibril sliding is indirectly measured in this study by changes in the variance of fibril *d*-periods, which would suggest

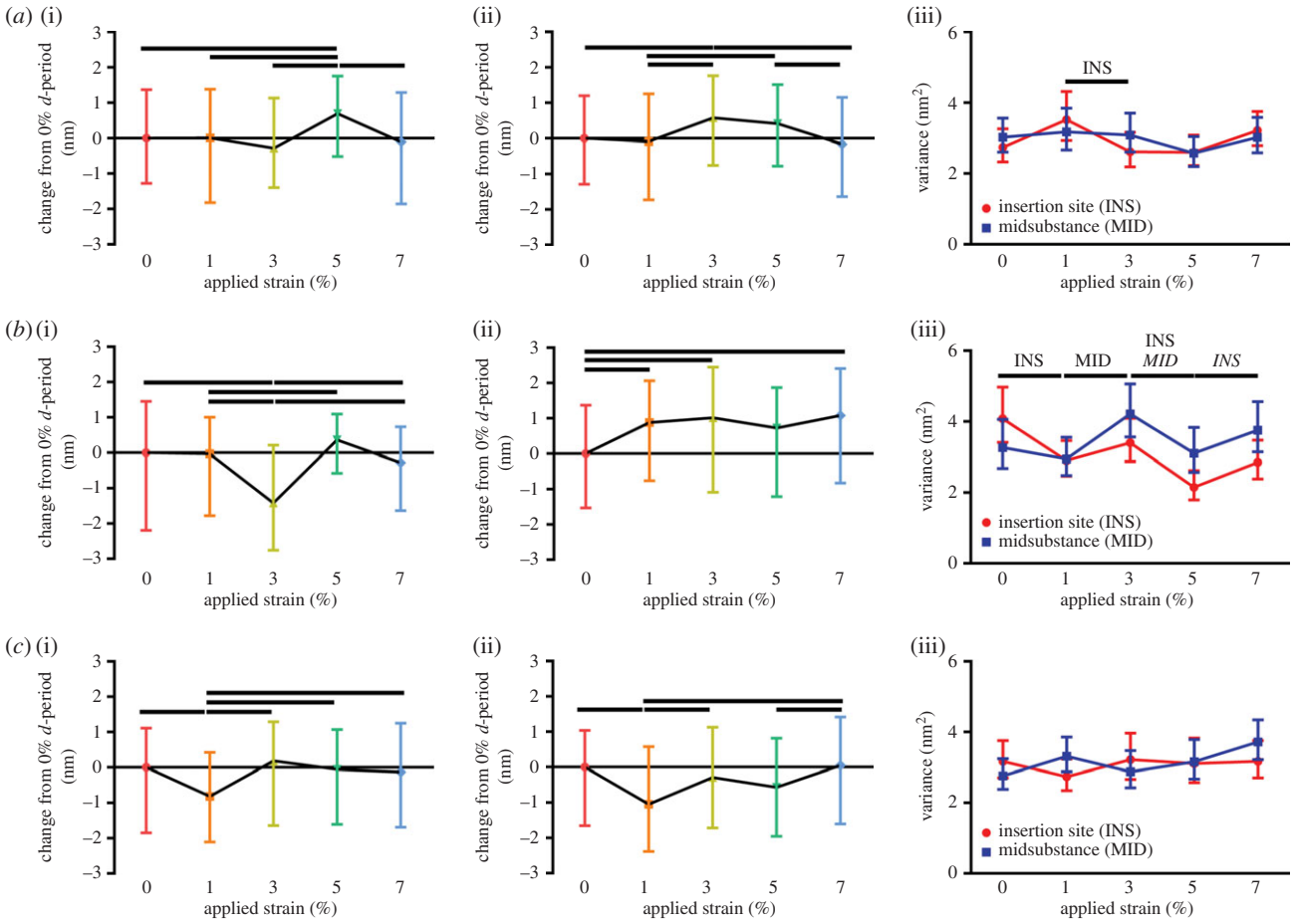

Figure 6. Results from fibril stretch at the insertion site (*a*(i), *b*(i) and *c*(i)) and midsubstance (*a*(ii), *b*(ii) and *c*(ii)) and fibril sliding at both locations (*a*(iii), *b*(iii) and *c*(iii)) are shown for each group. (*a*) The wild-type group exhibited an initial hold followed by an increase to 5% applied strain at the insertion site and a monotonic fibril stretch to peak at 3% applied strain at the midsubstance. Fibril sliding occurred in the insertion site from 1 to 3% applied strain. (*b*) The heterozygous group exhibited the same response as the wild-type group at the insertion site but earlier fibril strain at the midsubstance and significant fibril sliding at both locations throughout the test. (*c*) The null group exhibited an earlier response of fibril strain at the insertion site and a monotonic increase in strain following an initial reduction in strain at the midsubstance. No significant fibril sliding occurred in either of the null locations. Data are reported at median ± interquartile range. (Online version in colour.)

heterogeneity in fibril stretch and therefore fibril sliding. At the insertion site of the wild-type group, fibril sliding occurred in the insertion site between 1 and 3% applied strain (figure 6*a*(iii)). Contrary to our previous study [6], we did not find any significant fibril sliding occurring in the midsubstance of the wild-type group. In the heterozygous group, fibril sliding occurred between 0 and 1% applied strain at the insertion site, between 1 and 3% applied strain at the midsubstance, between 3 and 5% applied strain in both regions and between 5 and 7% applied strain at the insertion site (figure 6*b*(iii)). The null group did not exhibit any significant fibril sliding (figure 6*c*(iii)).

4. Discussion

This study measured the dynamic multiscale mechanical response of collagen V-heterozygous and -null SST tendons and determined the relationship between dynamic responses at multiple hierarchical scales (table 1). At the macroscale, almost every material parameter exhibited a dose-dependent decrease in properties as collagen V expression decreased from the wild-type to the heterozygous and null groups, particularly at high strains and high-frequency loading. This is consistent with several previous studies in multiple tendons [28,31,34]. Interestingly, there were few differences between the groups at low levels of strain, suggesting the heterozygous and null groups perform similarly to the wild-type group initially. Taken with larger failure strains in the heterozygous and null groups, these groups exhibit a longer, low stiffness stress–strain curve, which could support increased elasticity with low strain/low load exercise, as reported clinically. However, both experimental groups were also unable to withstand the same repetitive cyclic loading as the wild-type group, suggesting earlier damage accumulation due to inferior dynamic responses. While the null tendons were more viscoelastic initially and with low levels of strain (increased tangent delta, relaxation), the null tendons were unable to recover lost fluid during high and repetitive fatigue loading, resulting in early failure. The heterozygous group, which exhibited only small changes in many other macroscale properties, was significantly affected by the cyclic loading protocol, suggesting that the dynamic responses governing recovery from repetitive cyclic strain were diminished in this group [20,43,52–54].

As hypothesized, a larger diminished response at the microscale than the macroscale was revealed in both the heterozygous and null groups in the measures of collagen fibre re-organization. At the microscale, collagen fibre re-alignment occurred earlier or with a smaller application of strain in both

Table 1. Summary of key parameters. Data are presented at mean ± s.d. for all parameters except initial *d*-period and variance, which are presented as median ± interquartile range.

	body weight (g)	area (mm^2)	maximum stress (MPa)	stress relaxation (%)	cycles to failure
WT	30.3 ± 3.7[a,b]	0.13 ± 0.03[a,b]	34.6 ± 9.9[a]	35.5 ± 6.1	5336 ± 2849[b]
HET	28.7 ± 3.0[a]	0.12 ± 0.02[a]	33.2 ± 11.5[a]	39.5 ± 6.0	3117 ± 2068
NULL	18.2 ± 2.6	0.10 ± 0.03	13.9 ± 3.9	50.4 ± 9.9	1988 ± 1436
	dynamic modulus (MPa)	**tangent delta**	**tangent stiffness (N mm^{-1})**	**peak cyclic strain (%)**	**hysteresis (MPa mm mm^{-1})**
WT	194.8 ± 65.2[a]	0.04 ± 0.01[a]	17.8 ± 1.3[a,b]	1.4 ± 0.2	0.03 ± 0.01[a]
HET	160.4 ± 89.3	0.05 ± 0.01[a]	18.7 ± 1.6[a]	1.4 ± 0.1[a]	0.03 ± 0.008[a]
NULL	118.1 ± 52.0	0.06 ± 0.01	10.6 ± 1.3	1.5 ± 0.2	0.008 ± 0.003
	transition strain (%)	**transition stress (MPa)**	**toe modulus (MPa)**	**linear modulus (MPa)**	**initial *d*-period (nm)**
WT					
INS	5.3 ± 1.9	2.7 ± 1.5[a]	115.6 ± 64.9[a]	887.0 ± 435.3[a,b]	61.7 ± 2.7[b]
MID	4.3 ± 2.4	2.3 ± 1.8	122.3 ± 80.1[a,b]	713.7 ± 488.13[a]	62.0 ± 2.5[b]
HET					
INS	4.8 ± 1.3	1.8 ± 1.0	95.0 ± 46.4	616.9 ± 234.6[a]	62.5 ± 3.7[a]
MID	5.0 ± 2.0	1.9 ± 2.0	66.5 ± 68.6	549.3 ± 309.1[a]	61.3 ± 2.9[a]
NULL					
INS	5.0 ± 2.0	1.2 ± 1.0	53.1 ± 37.9	315.4 ± 183.5	62.0 ± 3.0
MID	5.5 ± 3.6	1.2 ± 1.0	41.8 ± 29.1	250.1 ± 106.4	62.2 ± 2.7
	toe region re-alignment	**linear region re-alignment**	**strain required to full re-align (%)**	**amount of re-alignment**	**initial variance (nm^2)**
WT					
INS	1.1 ± 0.7	0.9 ± 0.5[a,b]	5.2 ± 1.5	4.1 ± 1.4[a]	2.2 ± 1.0
MID	0.7 ± 0.7	0.5 ± 0.5[a]	5.9 ± 2.1[a]	2.4 ± 0.8	2.5 ± 1.6
HET					
INS	0.9 ± 0.5	0.4 ± 0.5	5.5 ± 1.6	3.8 ± 1.1	4.3 ± 2.5
MID	0.9 ± 0.8	0.7 ± 0.8	5.4 ± 1.5[a]	2.2 ± 1.0	2.9 ± 1.0
NULL					
INS	0.5 ± 0.9	0.2 ± 1.1	4.9 ± 1.6	2.7 ± 1.0	3.1 ± 1.2
MID	0.5 ± 1.0	0.2 ± 0.4	3.6 ± 1.4	2.6 ± 1.2	2.9 ± 2.0

[a] $p < 0.05$ with NULL.
[b] $p < 0.05$ with HET.

the heterozygous and null groups. While an earlier response to load could be seen as a positive trait, this also could suggest that the protection of fibrils from strain via other dynamic mechanisms is occurring earlier and subsequent damage can then accumulate in the tissue at a lower strain level. In fact, earlier re-alignment with decreased overall mechanical properties has been reported before in a mouse model of disease [55]. In addition, the null group re-aligned less than the wild-type group. Given no significant difference in the initial tissue organization was detected between groups, this suggests that the null group also has reduced capacity to re-align overall. Reduced ability to re-align could be associated with the lack of or deterioration of inter-fibre connectivity such as in development or ageing [5,36] or by alterations in the extrafibrillar matrix.

Furthermore, the heterozygous and null groups also exhibited an altered fibril response to load as well. Early structural re-organization resulting in fibril strain reduction at the insertion site appeared to be larger in the heterozygous group and earlier in the null group, confirming our results at the microscale. Furthermore, the fibrils also exhibited increased strain at an earlier applied strain level, implying an earlier response at the nanoscale. Unlike the wild-type group which exhibited a coordinated response of fibril stretch and sliding consistent with previous studies [6,7,56], the heterozygous and null groups had more unclear stretch/sliding relationships. This study revealed a significant amount of fibril sliding in the heterozygous group and no sliding in the null group. Both results (increased and decreased fibril sliding) imply that not only are the fibrils themselves altered by the reduction of collagen V expression during development, but that the interfibrillar matrix is most likely also altered [57,58].

With all of the multiscale results taken together, these results suggest different mechanisms by which the experimental groups attempt to withstand the same loading as the wild-type group. The wild-type group is able to reduce stress at the lower hierarchical scales (fibres, fibrils) through a series of coordinated dynamic responses, specifically collagen re-alignment and sliding. The heterozygous group compensates for the lack of fibril strength via earlier re-alignment and a large amount of fibril sliding. The sliding reduces strain on the collagen fibrils initially, and thus prevents early fibril failure, but with a large amount of repeated fibril sliding, the fibrils eventually pull away from each other and fail in shear, as is evidenced by reduced cycles to failure during fatigue loading. This allows the heterozygous group to respond elastically but only at low strain levels, which is consistent with clinical observations [28,32,59–61]. By contrast, the null group also responds early to load, but is incapable of producing significant fibril sliding, and therefore the tendons fail earlier and with lower maximum loads. These results provide insight into how structural alterations ultimately lead to functional deficiencies, particularly in the classic EDS patient population. While classic EDS patients may be able to perform reasonably during low impact activity, increased duration or magnitude could cause tendon damage which would ultimately lead to weakness, instability and injury.

While this study provides a unique set of multiscale mechanical parameters to understand hierarchical structure–function relationships, it is not without limitations. First and foremost, this study sought to investigate relationships between dynamic parameters but direct comparisons could not be made between these assays due to the inability to measure multiple hierarchical scales in a single measurement using the assays performed here. In addition, no compositional or structural measures are reported. This is particularly important as many of the dynamic responses studied here are functions of the innate structure and composition of the tissue. For example, the reduced fibril sliding found in the null group could be explained by increased stiffness of the extrafibrillar matrix, which would cause an increase in friction between fibrils. Similarly, increases of viscoelastic or elastic proteins (PGs or elastin, respectively) could be responsible for some of the mechanical changes found here. Ongoing studies are focused on measuring these changes in composition, organization and overall structure to investigate why these dynamic mechanical responses are altered.

Altogether, these studies highlight the relationships that exist between fibril, fibre and tissue-level mechanical function in the context of collagen V-heterozygous and -null tendons. Investigation into dynamic responses at the microscale and nanoscale could provide more information to elucidate the mechanisms by which mechanical function at the macroscale is ultimately altered. Furthermore, these studies suggest that these unique set of dynamic processes provide normal tendons with a series of protective measures to prevent early failure. It is likely that these mechanisms are the initiation of large-scale tissue damage, and ultimately this work could aid in the goal of improving tendon repair techniques or developing tissue-engineered constructs for tendon replacement.

Authors' contributions. B.K.C. has contributed to all aspects of this study, including research design, data acquisition, interpretation/analysis of data and drafting/revision of the manuscript. L.H., D.E.B. and L.J.S. have contributed significantly in research design, interpretation/analysis of data and drafting/revision of the manuscript. All authors have read and approved the final submitted manuscript.

Competing interests. We declare we have no competing interests.

Funding. This study was supported by NIH/NIAMS (T32-AR007132, AR044745 and AR065995) and the Penn Center for Musculoskeletal Disorders (NIH, P30 AR050950).

Acknowledgements. The authors acknowledge Benjamin Freedman, Joseph Sarver, Mei Sun, and Qingmei Yao for their assistance and technical expertise.

References

1. Connizzo BK, Yannascoli SM, Soslowsky LJ. 2013 Structure–function relationships of postnatal tendon development: a parallel to healing. *Matrix Biol.* **32**, 106–116. (doi:10.1016/j.matbio.2013.01.007)
2. Woo SL, Debski RE, Zeminski J, Abramowitch SD, Saw SS, Fenwick JA. 2000 Injury and repair of ligaments and tendons. *Annu. Rev. Biomed. Eng.* **2**, 83–118. (doi:10.1146/annurev.bioeng.2.1.83)
3. Hansen KA, Weiss JA, Barton JK. 2002 Recruitment of tendon crimp with applied tensile strain. *J. Biomech. Eng.* **124**, 72–77. (doi:10.1115/1.1427698)
4. Miller KS, Connizzo BK, Feeney E, Soslowsky LJ. 2012 Characterizing local collagen fiber re-alignment and crimp behavior throughout mechanical testing in a mature mouse supraspinatus tendon model. *J. Biomech.* **45**, 2061–2065. (doi:10.1016/j.jbiomech.2012.06.006)

5. Miller KS, Connizzo BK, Soslowsky LJ. 2012 Collagen fiber re-alignment in a neonatal developmental mouse supraspinatus tendon model. *Ann. Biomed. Eng.* **40**, 1102–1110. (doi:10.1007/s10439-011-0490-3)
6. Connizzo BK, Sarver JJ, Han L, Soslowsky LJ. 2014 *In situ* fibril stretch and sliding is location-dependent in mouse supraspinatus tendons. *J. Biomech.* **47**, 3794–3798. (doi:10.1016/j.jbiomech.2014.10.029)
7. Thorpe CT, Udeze CP, Birch HL, Clegg PD, Screen HR. 2013 Capacity for sliding between tendon fascicles decreases with ageing in injury prone equine tendons: a possible mechanism for age-related tendinopathy? *Eur. Cells Mater.* **25**, 48–60.
8. Rigozzi S, Stemmer A, Muller R, Snedeker JG. 2011 Mechanical response of individual collagen fibrils in loaded tendon as measured by atomic force microscopy. *J. Struct. Biol.* **176**, 9–15. (doi:10.1016/j.jsb.2011.07.002)
9. Diamant J, Keller A, Baer E, Litt M, Arridge RGC. 1972 Collagen; ultrastructure and its relation to mechanical properties as a function of ageing. *Proc. R. Soc. Lond. B* **180**, 293–315. (doi:10.1098/rspb.1972.0019)
10. Atkinson TS, Ewers BJ, Haut RC. 1999 The tensile and stress relaxation responses of human patellar tendon varies with specimen cross-sectional area. *J. Biomech.* **32**, 907–914. (doi:10.1016/S0021-9290(99)00089-5)
11. Rigozzi S, Muller R, Snedeker JG. 2009 Local strain measurement reveals a varied regional dependence of tensile tendon mechanics on glycosaminoglycan content. *J. Biomech.* **42**, 1547–1552. (doi:10.1016/j.jbiomech.2009.03.031)
12. Screen HR, Shelton JC, Chhaya VH, Kayser MV, Bader DL, Lee DA. 2005 The influence of noncollagenous matrix components on the micromechanical environment of tendon fascicles. *Ann. Biomed. Eng.* **33**, 1090–1099. (doi:10.1007/s10439-005-5777-9)
13. Dourte LM, Pathmanathan L, Jawad AF, Iozzo RV, Mienaltowski MJ, Birk DE, Soslowsky LJ. 2012 Influence of decorin on the mechanical, compositional, and structural properties of the mouse patellar tendon. *J. Biomech. Eng.* **134**, 031005. (doi:10.1115/1.4006200)
14. Dunkman AA *et al.* 2013 Decorin expression is important for age-related changes in tendon structure and mechanical properties. *Matrix Biol.* **32**, 3–13. (doi:10.1016/j.matbio.2012.11.005)
15. Elliott DM, Robinson PS, Gimbel JA, Sarver JJ, Abboud JA, Iozzo RV, Soslowsky LJ. 2003 Effect of altered matrix proteins on quasilinear viscoelastic properties in transgenic mouse tail tendons. *Ann. Biomed. Eng.* **31**, 599–605. (doi:10.1114/1.1567282)
16. Gautieri A, Vesentini S, Redaelli A, Buehler MJ. 2012 Viscoelastic properties of model segments of collagen molecules. *Matrix Biol.* **31**, 141–149. (doi:10.1016/j.matbio.2011.11.005)
17. Gimbel JA, Sarver JJ, Soslowsky LJ. 2004 The effect of overshooting the target strain on estimating viscoelastic properties from stress relaxation experiments. *J. Biomech. Eng.* **126**, 844–848. (doi:10.1115/1.1824132)
18. Screen HR. 2008 Investigating load relaxation mechanics in tendon. *J. Mech. Behav. Biomed. Mater.* **1**, 51–58. (doi:10.1016/j.jmbbm.2007.03.002)
19. Silver FH, Ebrahimi A, Snowhill PB. 2002 Viscoelastic properties of self-assembled type I collagen fibers: molecular basis of elastic and viscous behaviors. *Connect. Tissue Res.* **43**, 569–580. (doi:10.1080/03008200290001302)
20. Freedman BR, Sarver JJ, Buckley MR, Voleti PB, Soslowsky LJ. 2014 Biomechanical and structural response of healing Achilles tendon to fatigue loading following acute injury. *J. Biomech.* **47**, 2028–2034. (doi:10.1016/j.jbiomech.2013.10.054)
21. Einhorn TA, Buckwalter JA, O'Keefe RJ, American Academy of Orthopaedic Surgeons. 2007 *Orthopaedic basic science: foundations of clinical practice*. Rosemont, IL: American Academy of Orthopaedic Surgeons.
22. Birk DE, Nurminskaya MV, Zycband EI. 1995 Collagen fibrillogenesis in situ: fibril segments undergo post-depositional modifications resulting in linear and lateral growth during matrix development. *Dev. Dyn.* **202**, 229–243. (doi:10.1002/aja.1002020303)
23. Birk DE, Southern JF, Zycband EI, Fallon JT, Trelstad RL. 1989 Collagen fibril bundles: a branching assembly unit in tendon morphogenesis. *Development* **107**, 437–443.
24. Birk DE, Trelstad RL. 1986 Extracellular compartments in tendon morphogenesis: collagen fibril, bundle, and macroaggregate formation. *J. Cell Biol.* **103**, 231–240. (doi:10.1083/jcb.103.1.231)
25. Birk DE, Zycband EI, Woodruff S, Winkelmann DA, Trelstad RL. 1997 Collagen fibrillogenesis *in situ*: fibril segments become long fibrils as the developing tendon matures. *Dev. Dyn.* **208**, 291–298. (doi:10.1002/(SICI)1097-0177(199703)208:3<291::AID-AJA1>3.0.CO;2-D)
26. Woo SL, Thay QL, Abramowitch SD, Gilbert TW. 2005 Structure and function of ligaments and tendons. In *Basic orthopaedic biomechanics & mechano-biology*, pp. 301–342, 3rd edn. Philadelphia, PA: Lippincott, Williams & Wilkins.
27. Segev F *et al.* 2006 Structural abnormalities of the cornea and lid resulting from collagen V mutations. *Invest. Ophthalmol. Vis. Sci.* **47**, 565–573. (doi:10.1167/iovs.05-0771)
28. Wenstrup RJ, Florer JB, Davidson JM, Phillips CL, Pfeiffer BJ, Menezes DW, Chervoneva I, Birk DE. 2006 Murine model of the Ehlers–Danlos syndrome. col5a1 haploinsufficiency disrupts collagen fibril assembly at multiple stages. *J. Biol. Chem.* **281**, 12 888–12 895. (doi:10.1074/jbc.M511528200)
29. Wenstrup RJ, Smith SM, Florer JB, Zhang G, Beason DP, Seegmiller RE, Soslowsky LJ, Birk DE. 2011 Regulation of collagen fibril nucleation and initial fibril assembly involves coordinate interactions with collagens V and XI in developing tendon. *J. Biol. Chem.* **286**, 20 455–20 465. (doi:10.1074/jbc.M111.223693)
30. Wenstrup RJ, Florer JB, Brunskill EW, Bell SM, Chervoneva I, Birk DE. 2004 Type V collagen controls the initiation of collagen fibril assembly. *J. Biol. Chem.* **279**, 53 331–53 337. (doi:10.1074/jbc.M409622200)
31. Sun M, Connizzo BK, Adams SM, Freedman BR, Wenstrup RJ, Soslowsky LJ, Birk DE. 2015 Targeted deletion of collagen V in tendons and ligaments results in a classic Ehlers–Danlos syndrome joint phenotype. *Am. J. Pathol.* **185**, 1436–1447. (doi:10.1016/j.ajpath.2015.01.031)
32. Malfait F, Coucke P, Symoens S, Loeys B, Nuytinck L, De Paepe A. 2005 The molecular basis of classic Ehlers–Danlos syndrome: a comprehensive study of biochemical and molecular findings in 48 unrelated patients. *Hum. Mutat.* **25**, 28–37. (doi:10.1002/humu.20107)
33. Symoens S, Syx D, Malfait F, Callewaert B, De Backer J, Vanakker O, Coucke P, De Paepe A. 2012 Comprehensive molecular analysis demonstrates type V collagen mutations in over 90% of patients with classic EDS and allows to refine diagnostic criteria. *Hum. Mutat.* **33**, 1485–1493. (doi:10.1002/humu.22137)
34. Connizzo BK, Freedman BR, Fried JH, Sun M, Birk DE, Soslowsky LJ. 2015 Regulatory role of collagen V in establishing mechanical properties of tendons and ligaments is tissue-dependent. *J. Orthop. Res.* **33**, 882–888. (doi:10.1002/jor.22893)
35. Sun M, Chen S, Adams SM, Florer JB, Liu H, Kao WW, Wenstrup RJ, Birk DE. 2011 Collagen V is a dominant regulator of collagen fibrillogenesis: dysfunctional regulation of structure and function in a corneal-stroma-specific Col5a1-null mouse model. *J. Cell Sci.* **124**, 4096–4105. (doi:10.1242/jcs.091363)
36. Connizzo BK, Sarver JJ, Birk DE, Soslowsky LJ, Iozzo RV. 2013 Effect of age and proteoglycan deficiency on collagen fiber re-alignment and mechanical properties in mouse supraspinatus tendon. *J. Biomech. Eng.* **135**, 021019. (doi:10.1115/1.4023234)
37. Derwin KA, Soslowsky LJ, Green WD, Elder SH. 1994 A new optical system for the determination of deformations and strains: calibration characteristics and experimental results. *J. Biomech.* **27**, 1277–1285. (doi:10.1016/0021-9290(94)90281-X)
38. Beason DP, Hsu JE, Marshall SM, McDaniel AL, Temel RE, Abboud JA, Soslowsky LJ. 2013 Hypercholesterolemia increases supraspinatus tendon stiffness and elastic modulus across multiple species. *J. Shoulder Elbow Surg.* **22**, 681–686. (doi:10.1016/j.jse.2012.07.008)
39. Carpenter JE, Thomopoulos S, Flanagan CL, DeBano CM, Soslowsky LJ. 1998 Rotator cuff defect healing: a biomechanical and histologic analysis in an animal model. *J. Shoulder Elbow Surg.* **7**, 599–605. (doi:10.1016/S1058-2746(98)90007-6)
40. Dourte LM, Pathmanathan L, Mienaltowski MJ, Jawad AF, Birk DE, Soslowsky LJ. 2013 Mechanical, compositional, and structural properties of the mouse patellar tendon with changes in biglycan

gene expression. *J. Orthop. Res.* **31**, 1430–1437. (doi:10.1002/jor.22372)

41. Ansorge HL, Adams S, Birk DE, Soslowsky LJ. 2011 Mechanical, compositional, and structural properties of the post-natal mouse Achilles tendon. *Ann. Biomed. Eng.* **39**, 1904–1913. (doi:10.1007/s10439-011-0299-0)
42. Dunkman AA *et al.* 2014 The injury response of aged tendons in the absence of biglycan and decorin. *Matrix Biol.* **35**, 232–238. (doi:10.1016/j.matbio.2013.10.008)
43. Freedman BR, Zuskov A, Sarver JJ, Buckley MR, Soslowsky LJ. 2015 Evaluating changes in tendon crimp with fatigue loading as an ex vivo structural assessment of tendon damage. *J. Orthop. Res.* **33**, 904–910. (doi:10.1002/jor.22875)
44. Duenwald-Kuehl S, Kondratko J, Lakes RS, Vanderby Jr R. 2012 Damage mechanics of porcine flexor tendon: mechanical evaluation and modeling. *Ann. Biomed. Eng.* **40**, 1692–1707. (doi:10.1007/s10439-012-0538-z)
45. Provenzano PP, Heisey D, Hayashi K, Lakes R, Vanderby JR R. 2002 Subfailure damage in ligament: a structural and cellular evaluation. *J. Appl. Physiol. (1985)* **92**, 362–371.
46. Lake SP, Miller KS, Elliott DM, Soslowsky LJ. 2009 Effect of fiber distribution and realignment on the nonlinear and inhomogeneous mechanical properties of human supraspinatus tendon under longitudinal tensile loading. *J. Orthopaed. Res.* **27**, 1596–1602. (doi:10.1002/jor.20938)
47. Lake SP, Miller KS, Elliott DM, Soslowsky LJ. 2010 Tensile properties and fiber alignment of human supraspinatus tendon in the transverse direction demonstrate inhomogeneity, nonlinearity, and regional isotropy. *J. Biomech.* **43**, 727–732. (doi:10.1016/j.jbiomech.2009.10.017)
48. Miller KS, Connizzo BK, Feeney E, Tucker JJ, Soslowsky LJ. 2012 Examining differences in local collagen fiber crimp frequency throughout mechanical testing in a developmental mouse supraspinatus tendon model. *J. Biomech. Eng.* **134**, 041004. (doi:10.1115/1.4006538)
49. Miller KS, Edelstein L, Connizzo BK, Soslowsky LJ. 2012 Effect of preconditioning and stress relaxation on local collagen fiber re-alignment: inhomogeneous properties of rat supraspinatus tendon. *J. Biomech. Eng.* **134**, 031007. (doi:10.1115/1.4006340)
50. Thomas S, Miller KS, Soslowsky LJ. 2012 The upper band of the subscapularis tendon in the rat has altered mechanical and histologic properties. *J. Shoulder Elbow Surg.* **21**, 1687–1693. (doi:10.1016/j.jse.2011.11.038)
51. Rigozzi S, Muller R, Stemmer A, Snedeker JG. 2013 Tendon glycosaminoglycan proteoglycan sidechains promote collagen fibril sliding—AFM observations at the nanoscale. *J. Biomech.* **46**, 813–818. (doi:10.1016/j.jbiomech.2012.11.017)
52. Shepherd JH, Riley GP, Screen HR. 2014 Early stage fatigue damage occurs in bovine tendon fascicles in the absence of changes in mechanics at either the gross or micro-structural level. *J. Mech. Behav. Biomed. Mater.* **38**, 163–172. (doi:10.1016/j.jmbbm.2014.06.005)
53. Thorpe CT, Riley GP, Birch HL, Clegg PD, Screen HR. 2014 Effect of fatigue loading on structure and functional behaviour of fascicles from energy-storing tendons. *Acta Biomater.* **10**, 3217–3224. (doi:10.1016/j.actbio.2014.04.008)
54. Thorpe CT, Riley GP, Birch HL, Clegg PD, Screen HR. 2014 Fascicles from energy-storing tendons show an age-specific response to cyclic fatigue loading. *J. R. Soc. Interface* **11**, 20131058. (doi:10.1098/rsif.2013.1058)
55. Connizzo BK, Bhatt PR, Liechty KW, Soslowsky LJ. 2014 Diabetes alters mechanical properties and collagen fiber re-alignment in multiple mouse tendons. *Ann. Biomed. Eng.* **42**, 1880–1888. (doi:10.1007/s10439-014-1031-7)
56. Szczesny SE, Elliott DM. 2014 Interfibrillar shear stress is the loading mechanism of collagen fibrils in tendon. *Acta Biomater.* **10**, 2582–2590. (doi:10.1016/j.actbio.2014.01.032)
57. Thorpe CT, Birch HL, Clegg PD, Screen HR. 2013 The role of the non-collagenous matrix in tendon function. *Int. J. Exp. Pathol.* **94**, 248–259. (doi:10.1111/iep.12027)
58. Thorpe CT, Udeze CP, Birch HL, Clegg PD, Screen HR. 2012 Specialization of tendon mechanical properties results from interfascicular differences. *J. R. Soc. Interface* **9**, 3108–3117. (doi:10.1098/rsif.2012.0362)
59. Castori M, Sperduti I, Celletti C, Camerota F, Grammatico P. 2011 Symptom and joint mobility progression in the joint hypermobility syndrome (Ehlers–Danlos syndrome, hypermobility type). *Clin. Exp. Rheumatol.* **29**, 998–1005.
60. Nielsen RH *et al.* 2014 Low tendon stiffness and abnormal ultrastructure distinguish classic Ehlers–Danlos syndrome from benign joint hypermobility syndrome in patients. *FASEB J.* **28**, 4668–4676. (doi:10.1096/fj.14-249656)
61. Nordschow CD, Marsolais EB. 1969 Ehlers–Danlos syndrome. Some recent biophysical observations. *Arch. Pathol.* **88**, 65–68.